Transcriptional and cell type profiles of cortical brain regions showing ultradian cortisol rhythm dependent responses to emotional face stimulation

Habets, P.C.; Kalafatakis, K.; Dzyubachyk, O.; Werff, S.J.A. van der; Keo, A.; Thakrar, J.; ... ; Meijer, O.C.

Neurobiology of Stress 22 (2023) 100514

Contents lists available at ScienceDirect

Neurobiology of Stress

journal homepage: www.elsevier.com/locate/ynstr

Transcriptional and cell type profiles of cortical brain regions showing ultradian cortisol rhythm dependent responses to emotional face stimulation

Philippe C. Habets [a,b,*], Konstantinos Kalafatakis [c,d], Oleh Dzyubachyk [e,f], Steven J.A. van der Werff [g,h], Arlin Keo [i,j], Jamini Thakrar [c], Ahmed Mahfouz [i,j,k], Alberto M. Pereira [a,l], Georgina M. Russell [c], Stafford L. Lightman [c], Onno C. Meijer [a,h]

[a] Leiden University Medical Center, Department of Medicine, Division of Endocrinology, 2300 RC Leiden, the Netherlands
[b] Amsterdam University Medical Centre, Department of Psychiatry, Department of Anatomy and Neurosciences, 1081 HZ, Amsterdam, the Netherlands
[c] Henry Wellcome Laboratories of Integrative Neuroscience and Endocrinology, Bristol Medical School, University of Bristol, BS1 3NY, Bristol, United Kingdom
[d] Institute of Health Sciences Education, Barts and the London School of Medicine & Dentistry, Queen Mary University of London Malta Campus, VCT 2520, Victoria Gozo, Malta
[e] Department of Radiology, Division of Medical Image Processing, Leiden University Medical Center, 2333 ZA, Leiden, the Netherlands
[f] Leiden University Medical Center, Department of Cell and Chemical Biology, Section Electron Microscopy, 2300 RC, Leiden, the Netherlands
[g] Department of Psychiatry, Leiden University Medical Center LUMC, Leiden, the Netherlands
[h] Leiden Institute for Brain and Cognition, Leiden, the Netherlands
[i] Leiden Computational Biology Center, Leiden University Medical Center, Leiden, the Netherlands
[j] Delft Bioinformatics Lab, Delft University of Technology, Delft, the Netherlands
[k] Department of Human Genetics, Leiden University Medical Center, Leiden, the Netherlands
[l] Department of Endocrinology & Metabolism, Amsterdam University Medical Center, Amsterdam, the Netherlands

ARTICLE INFO

Keywords:
fMRI
Transcriptomics
Brain
Allen human brain atlas

ABSTRACT

The characteristic endogenous circadian rhythm of plasma glucocorticoid concentrations is made up from an underlying ultradian pulsatile secretory pattern. Recent evidence has indicated that this ultradian cortisol pulsatility is crucial for normal emotional response in man. In this study, we investigate the anatomical transcriptional and cell type signature of brain regions sensitive to a loss of ultradian rhythmicity in the context of emotional processing. We combine human cell type and transcriptomic atlas data of high spatial resolution with functional magnetic resonance imaging (fMRI) data. We show that the loss of cortisol ultradian rhythm alters emotional processing response in cortical brain areas that are characterized by transcriptional and cellular profiles of GABAergic function. We find that two previously identified key components of rapid non-genomic GC signaling – the ANXA1 gene and retrograde endocannabinoid signaling – show most significant differential expression ($q = 3.99e^{-10}$) and enrichment (fold enrichment = 5.56, $q = 9.09e^{-4}$). Our results further indicate that specific cell types, including a specific NPY-expressing GABAergic neuronal cell type, and specific G protein signaling cascades underly the cerebral effects of a loss of ultradian cortisol rhythm. Our results provide a biological mechanistic underpinning of our fMRI findings, indicating specific cell types and cascades as a target for manipulation in future experimental studies.

1. Introduction

Glucocorticoids (GCs) are a class of mammalian hormones known for their pleotropic effects across different bodily systems, such as metabolism, fluid homeostasis, immune and stress system responsivity, as well as brain function. The immunomodulatory capacity of these hormones has been utilized in clinical therapeutics for more than half a century (Rhen and Cidlowski, 2005). The underlying mechanisms through which GCs mediate such a diversity of biological processes remain a topic of intensive investigation. Recent evidence indicates that biorhythmicity might be of great importance. GCs exhibit a circadian rhythm, with high hormonal levels being secreted just prior to and

* Corresponding author. Leiden University Medical Center, Department of Medicine, Division of Endocrinology, 2300 RC Leiden, the Netherlands.
E-mail addresses: p.c.habets@lumc.nl, p.c.habets@amsterdamumc.nl (P.C. Habets), a.m.pereiraarias@amsterdamumc.nl (A.M. Pereira).

https://doi.org/10.1016/j.ynstr.2023.100514
Received 14 September 2022; Received in revised form 2 January 2023; Accepted 2 January 2023
Available online 4 January 2023

during the active part of the day. The circadian rhythm is superimposed on an underlying ultradian rhythm of more frequent episodes of GC secretion (i.e., hormonal pulses) (Russell et al., 2015). The brain is exposed to these hormonal pulses and has developed mechanisms able to perceive them and translate them to cellular, genomic and non-genomic events (Kalafatakis et al., 2019; Sarabdjitsingh et al., 2010). Thus, GC pulsatility might regulate various physiological -, neural -, and glial processes, under baseline and stressful conditions, and hormonal dysrhythmicity could be associated with cognitive and behavioural disorders (Kalafatakis et al., 2021; Sarabdjitsingh et al., 2010).

We designed and conducted a randomised, double-blind, placebo-controlled, crossover study to assess functional relevance of GC pulsatility for human brain circuitry. We used a human model of adrenal insufficiency (metyrapone-induced suppression of GC endogenous biosynthesis) (Kalafatakis et al., 2016), in which GC deficiency was exogenously replaced via two different, pump-mediated subcutaneous infusion methods: one mimicking the normal adrenal function under baseline conditions (resembling the normal circadian and underlying ultradian, pulsatile rhythm) and another lacking GC ultradian pulsatility. The cumulative dosage of the infused hydrocortisone was equal for both methods (20 mg/day). Exposure of the human brain to the same emotional stimuli (fearful, happy, and sad faces) provoked a differential response from corticolimbic regions of the right hemisphere, involved in emotional processing, depending on the mode (i.e., presence or absence of ultradian rhythmicity) of GC replacement (Kalafatakis et al., 2018). These functional magnetic resonance imaging (MRI) findings provide evidence that ultradian GC rhythm could be critical in regulating neural dynamics in human, but, at the same time, they raise the question of why these particular brain regions are sensitive to changes in GC rhythmicity, while other brain regions are not.

In the current work, we approached this question from a transcriptional and cell type point of view: we investigated the relationship between differential GC rhythm-dependent brain activation in the fMRI data and anatomically patterned transcriptional and cell type profiles. To do this we utilized available data from the Allen Human Brain Atlas (AHBA) (Hawrylycz et al., 2012). This is an anatomically comprehensive transcriptional brain atlas sampled from a number of carefully selected, clinically unremarkable donor brains, produced by a combination of histology-guided fine neuroanatomical molecular profiling and microarray-assisted mapping of gene expression data into MRI coordinate space. The AHBA provides an unparalleled high-resolution genome-wide map of transcript distribution and the ability to analyze genes underlying the function of specific brain regions (Bauduin et al., 2021; Burt et al., 2018; Habets et al., 2021; Li et al., 2021; Meijer et al., 2021).

In this context, we combined the functional MRI results of our study with available AHBA data to investigate which genes of the AHBA donor brains were differentially expressed in the GC rhythm-sensitive cortical brain areas (as specified by our functional MRI study) in comparison with the remaining cortical areas, thus specifying an anatomical transcriptomic signature of GC rhythm-sensitive cortical brain areas. We utilized gene ontology, pathway and protein-protein interaction databases to look for enrichment of functions (i.e., relate gene expression profiles of brain GC rhythm sensitivity to enrichment of specific brain cell functionality). We also utilized AHBA neuronal cell type databases to scale up the signature of cortical brain GC rhythm sensitivity from a transcript to a cell type level. In the latter case, if specific human-verified neuronal cell types are discovered to be enriched in the areas that show GC rhythm-responsivity, this could trigger a selective, preclinical, experimental investigation on the relationship between these human neuronal cell types and GC rhythmicity.

2. Materials and methods

2.1. Functional MRI study

This was a randomized, double-blind, placebo-controlled crossover study of different modes of hydrocortisone replacement in healthy subjects, registered with the United Kingdom Clinical Research Network (IRAS reference 106181, UKCRN-ID-15236; October 23, 2013). The study followed the CONSORT guidelines for randomized controlled trials. Fifteen right-handed, healthy male volunteers aged 20–33 years were included in the study. The Ethics Committee of the University of Bristol approved the study, and all participants provided informed written consent. More details on the development and validation of the human model of adrenal insufficiency, and the different modes of GC replacement therapy, inclusion and exclusion criteria of the study, recruitment process, quality control and bioethical concerns, randomization, and blinding processes, as well a detailed presentation of all outcome measures recruited (aside functional MRI), can be found elsewhere (Kalafatakis et al., 2016, 2018, 2021).

2.2. Functional MRI data

The functional image pre-processing steps consisted of (i) brain intensity normalization, (ii) 3D motion correction, (iii) B_0 unwarping with assistance from the B_0 fieldmap images, (iv) brain extraction, (v) spatial smoothing, (vi) temporal high pass filtering, and (vii) co-registration of the functional image with a corresponding high-resolution, anatomical, T_1-weighted image and with MNI152 standard space. Bias field correction has been applied, before removing the non-brain tissue from the high-resolution image. For each individual/session functional MRI dataset, a regression analysis was performed using a general linear model fitting the temporal evolution corresponding to the paradigm (emotional face presentation). A fraction of the temporal derivative of the blurred original waveform was added to the model. Temporal filtering was also applied. The form of the hemodynamic response function convolution method applied to the basic waveform was the Gamma variate. Three different effects were modelled (original exploratory variables); visual exposure to (i) fearful human faces, (ii) happy human faces and (iii) sad human faces. For the statistical analysis of the functional MRI data acquired during the presentation of emotional faces, we produced individual session/subject level maps of activity, indicating which brain regions were responding to the emotional face recognition (contrasting the baseline, resting state condition). For the comparisons between the GC pulsatile and non-pulsatile groups, whole-brain, group-level analyses were carried out using a mixed effects model. Each group-level analysis produced thresholded z-score brain region clusters highlighting statistically significant variations in the activation pattern between the GC pulsatile and non-pulsatile groups in response to emotional face stimulation. In all cases, corrections for multiple comparisons were performed at the cluster level using Gaussian random field theory (minimum $z > 2.3$, cluster p threshold <0.05) (Kalafatakis et al., 2018).

2.3. Transcriptomic atlas

The Allen Human Brain Atlas (AHBA) is a publicly available transcriptional atlas based on microarray measures, using a set of 58692 probes in 3702 samples across brainstem, cerebellum, subcortical and cortical brain structures across six postmortem human brains (five males and one female, age range 24–57, African American, Caucasian and Hispanic ethnicities). For limited samples of two donor brains, expression values were also measured by RNA sequencing. All expression data and metadata were downloaded from the AHBA (http://human.brain-map.org) on October 14th, 2019.

2.4. Data analysis

Our data analysis method can be summarized into seven distinct steps (see below). Many of our choices for data handling have been based on the work of Arnatkeviciute et al. (Arnatkeviciute et al., 2019). For step two (probe selection) and part of step three (sample selection), MATLAB scripts from their processing pipeline (publicly available at https://github.com/BMHLab/AHBAprocessing/) were adapted and customized for our own analysis (with their approval), using MATLAB version R2020a. For the rest of the analysis steps, except for probe reannotation, the programming language R (version 3.6) has been utilized. All used R packages were installed under R build 3.6. All R code is made publicly available on GitHub at https://github.com/pchabets/fMRI-transcriptomics-cortisol.

Step 1. Reannotation of probes

Since the probe annotation originally provided by the Allen Institute dates from a decade ago, probes were first reannotated to the latest human genome version and reference sequence using the Re-Annotator pipeline (Arloth et al., 2015). Re-Annotator is freely available for download at https://sourceforge.net/projects/reannotator/. The most recent genome and reference sequence were downloaded from the UCSC website on May 20th, 2020. The reannotation step resulted in the selection of 46,039 probes annotated to a total of 20,200 unique genes for inclusion into further analysis.

Step 2. Probe selection

If multiple probes were annotated to the same gene, we selected the best representative probe for that gene. Previous work has shown that selecting probes on the basis of the highest expression (intensity based filtering) improves the mean correlation between microarray and RNA sequencing (RNAseq) measures of gene expression obtained in the same brain samples, and increases the average inter-probe correlation for individual genes, thus improving microarray data reliability (Arnatkeviciute et al., 2019). Therefore, we first selected probes that showed a signal above noise signal in at least 50% of cortical and subcortical samples across all subjects (cf. Fig. 3A of Arnatkeviciute et al., 2019). This resulted in 31977 remaining probes, annotated to 15719 unique genes. Next, for each gene, if multiple probes were annotated to that gene, one single probe was selected by choosing the probe with the highest correlation to the RNAseq measures for the same gene in the same samples (RNA sequencing data available for first two donors. Data were downloaded at http://human.brain-map.org/static/download on October 14th, 2019). To further improve reliability of the differential expression analysis based on microarray probe measurements, we removed probes from the analysis that: a) were annotated to a gene that was not detected by the RNAseq measurement in the same sample, b) showed a low correlation to RNAseq data (Spearman Rho <0.2). This resulted in 10014 probes selected for 10014 unique genes. Previous work showed that functional enrichment analysis of genes that are removed based on these criteria show no enrichment for genes related to neuronal function (Arnatkeviciute et al., 2019).

Step3. Sample selection

Two AHBA donor brains were sampled bilaterally, while the other four donor brains were only profiled on the left hemisphere. This was done because no significant interhemispheric transcriptional difference was found in the first two brains. This is in accordance with previous evidence indicating that indeed no statistically significant transcriptomic differences between the left and right hemispheres exist (Hawrylycz et al., 2012; Johnson et al., 2009). To maximize spatial coverage, we only included AHBA samples from the left cerebral cortex for analysis. Because the differentially responding brain regions in the considered fMRI data were located on the right hemisphere, we symmetrically flipped the MNI-coordinates of the affected brain regions from right to left, to optimize spatial transcriptomic coverage. Flipping the fMRI mask from right to left is a valid approach in this case, since we are looking at cortical anatomical transcriptional patterning only, and no statistically significant hemispheric difference exists on the mRNA level.

Left hemisphere samples were selected if they could be annotated to the Desikan cortical parcellation atlas, using the AHBA processing pipeline available at https://github.com/BMHLab/AHBAprocessing/(Desikan et al., 2006). In total, 1285 left cortical samples were included for differential gene expression analysis. Next, AHBA samples and fMRI masks were plotted in MNI152 space. Using trilinear interpolation, it was calculated for each AHBA sample whether it could be assigned to an "affected" brain area (meaning falling inside either of the two fMRI thresholded masks) or not. This resulted in 61 samples in the "affected" brain regions versus 1224 samples in the "unaffected" brain regions.

Step 4. Normalization of expression values

Variations in the way tissue samples were acquired, handled and processed – e.g. brain pH, post-mortem interval and RNA degradation – can potentially affect gene expression measurements. The Allen Institute has implemented a series of steps to mitigate this variability as much as possible, as outlined in the Allen Human Brain Atlas technical white paper ("Technical White Paper: Microarray Data Normalization," 2013). Despite the measures implemented by the Allen Institute, Arnatkeviciute et al. (Neuroimage, 2019), have shown that, while the data normalization procedures applied by the Allen Institute prior to data release removed batch effects and artefactual inter-individual differences, a considerable degree of intrinsic donor-specific variance remains, and must be accounted for in order to perform valid data aggregation (we reiterated this finding by using unsupervised tSNE projection of the 1285 left cortical samples in the plot in Fig. 1C). The tSNE plot clearly showed clustering of samples by donor brain. We therefore corrected for possible donor-driven effects by using the *RemoveBatchEffect* function from the limma package for R (Ritchie et al., 2015), treating each donor as a separate batch. Because the limma function uses linear modelling, this correction method can be sensitive to outliers. Therefore, an additional outlier-robust normalization strategy was performed using scaled robust sigmoid (SRS) normalization:

$$x_y = \frac{1}{1+\exp\left(\frac{-(x_i-\langle x\rangle)}{IQR/1.35}\right)}$$

where $\langle x\rangle$ and IQR represent the median and the inter-quartile range respectively,

Followed by rescaling to a unit interval of 0–1 (Arnatkeviciute et al., 2019; Fulcher et al., 2013):

$$x_{norm} = \frac{x_y - \min(x)}{\max(x) - \min(x)}$$

Fig. 1C shows the effect of this normalization strategy on the donor-driven clustering of samples. To also account for gene outliers within each sample due to sample-specific artefacts, we additionally performed the same SRS and unit-interval scaling procedure within each sample, across all the measured gene expressions (within-sample, across-genes normalization). Lastly, we used a mixed linear modelling approach to model in any remaining donor driven effects (see *step 5* below).

Step 5. Testing significance of differentially expressed genes

Differential gene expression analysis between the 61 "affected" versus 1224 "unaffected" samples was performed using the limma package for R (Ritchie et al., 2015). Genes were ranked in order of evidence for differential expression by first fitting a linear model to the microarray data with the *lmFit* function, and then using an empirical Bayes method to shrink the probe-wise sample variances towards a common value and to augmenting the degrees of freedom for the individual variances with the *eBayes* function (Ritchie et al., 2015; Smyth, 2004). To further correct for the fact that samples in the "affected" and "unaffected" regions came from the same six donor brains, we included a

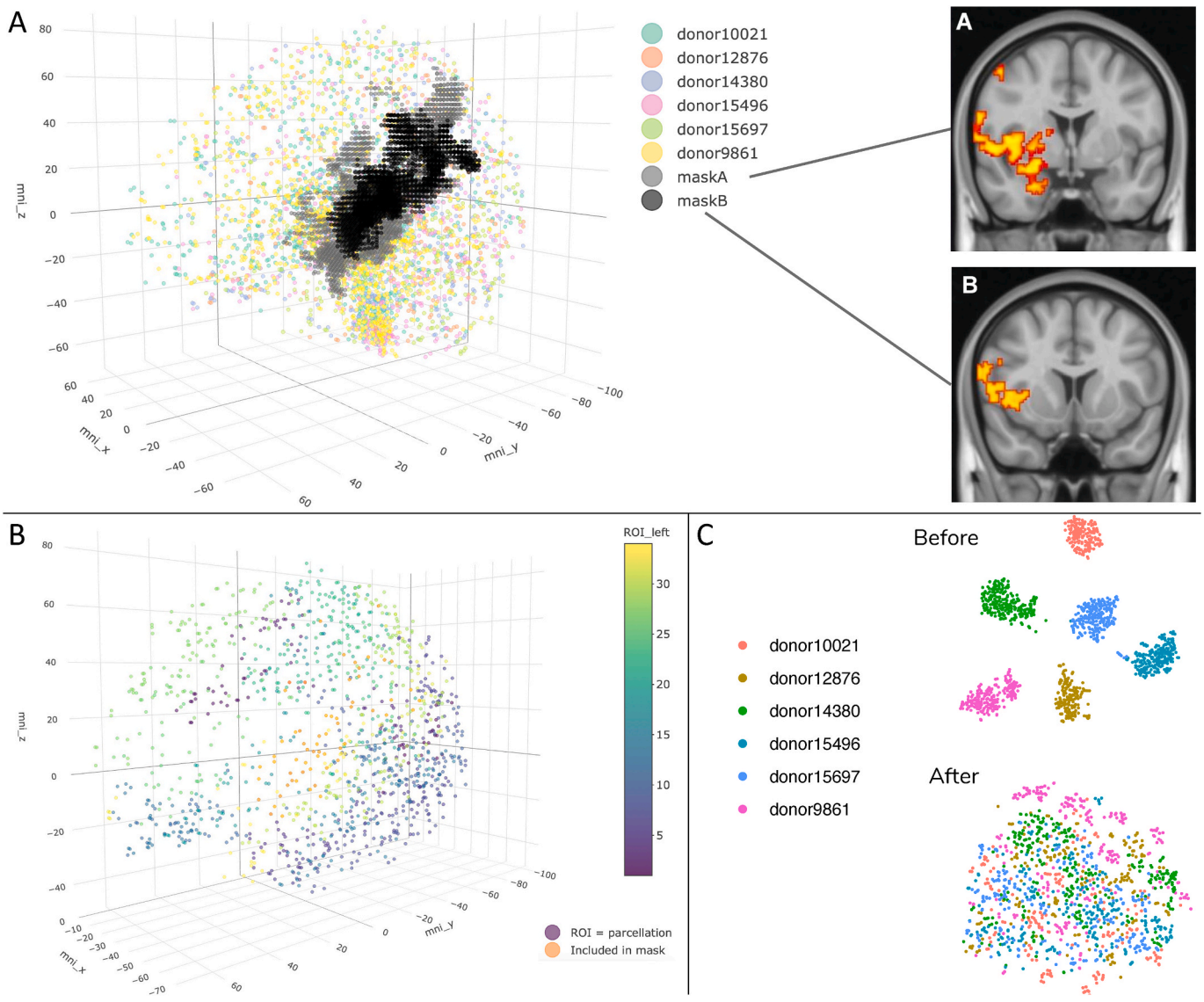

Fig. 1. A. 3702 AHBA brain samples plotted with left-mapped brain regions that show differential responsiveness to GC pulsatility in the same three-dimensional (MNI-152) space. "Mask A″ and "mask B" (black and grey dots in the 3D plot) correspond to the left-mapped versions of the brain regions that show differential responsiveness to GC pulsatility in the right hemisphere (2D images A & B). **B.** 1285 left cortical samples included in the differential expression analysis. Samples are colored depending on the Desikan parcellation they are mapped to (34 parcellations in total). Samples included in the mirrored fMRI mask coordinates (A and B from Fig. 1) are presented in orange. **C.** tSNE on the 1285 included left cortical samples before (left) and after (right) applying our normalization strategy (see Methods section for details). . (For interpretation of the references to color in this figure legend, the reader is referred to the Web version of this article.)

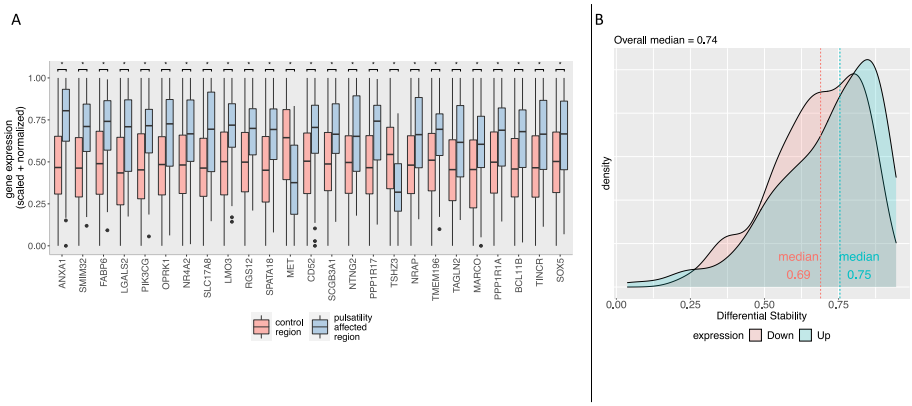

Fig. 2. A. Boxplot of top 25 differentially expressed genes, ordered by significance from left to right (increasing p-value from left to right). The bottom and top hinges correspond to the first and third quartiles, with the median shown in the interquartile range (IQR). Whiskers extend to the smallest and largest values within a range of 1.5*IQR from the bottom or top hinge. Values outside the 1.5*IQR range are plotted as individual outliers. All plotted results have FDR corrected $p < 0.05$ (*). A list of all differentially expressed genes is included as extended data in Table S2. **B.** Density plot of differential stability values, plotted separately for higher and lower differentially expressed genes.

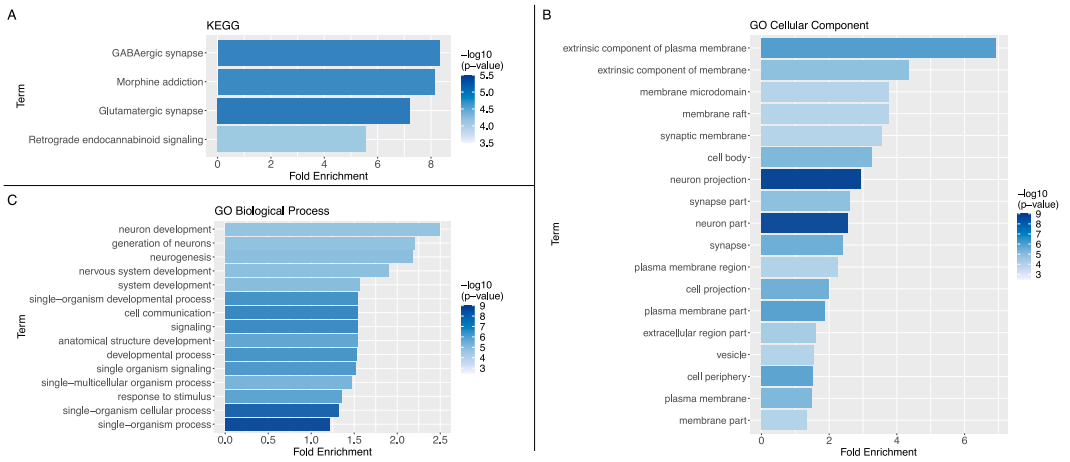

Fig. 3. Functional enrichment analysis results for **A)** KEGG pathways, **B)** GO categories relating to cellular components and **C)** GO categories relating to biological processes. Only term enrichments with Bonferroni-adjusted $p < 0.05$ are shown. Terms are ordered according to fold enrichment relative to chance, with colours indicating the -$\log_{10}$() transformed nominal p-value (higher -$\log_{10}$() value means lower p-value). Additional enrichment analysis using the PheWeb database is included in the extended data as Fig. S1. Data of the GO and KEGG enrichment analyses for both higher and lower differentially expressed genes are included in the extended data as Table S3 (for higher expressed genes) and Table S4 (for lower expressed genes). Enrichment analysis of psychiatric disease transcriptomic signatures is included as extended data in Table S5. . (For interpretation of the references to color in this figure legend, the reader is referred to the Web version of this article.)

correlation term for samples coming from the same donor brain using the *duplicateCorrelation* function. We passed this as argument in the *lmFit* function before passing the resulting fit to the *eBayes* function to allow for repeated measures from the same subjects, by using a mixed linear model that accounts for any remaining donor effects.

False discovery rate correction was performed by using the Benjamini-Hochberg (BH) procedure. BH-corrected p-values of $p < 0.05$ were considered significant. To check reproducible gene expression patterns of these differentially expressed genes across all donor brains – meaning across all donor brains regardless of sex, age and other donor related factors (see Table S1 for descriptives, and more detailed technical information in the technical white paper ("Technical White Paper: Microarray Data Normalization," 2013)) –, we cross-referenced publicly available results of calculated differential stability (DS) metrics for the same AHBA data (Supplementary Table 2 of the study by Hawrylycz et al. (2015)), plotting the distribution of DS values for the differentially expressed genes (see Fig. 2B). Differential stability is a correlation-based measure for the consistency of a gene's differential expression pattern across brain structures (Shaw et al., 2011). A difference in median differential stability of the differentially expressed genes in comparison with other genes was tested using the Mann-Whitney *U* test.

Step 6. Functional and protein-protein interaction enrichment analysis

Functional enrichment analysis of differentially expressed genes was performed using the RDAVIDWebService package for R (Fresno and Fernández, 2013). Gene ontology terms for biological processes, molecular function and cellular components, as well as pathways described in the KEGG database, were considered. As a background, the transcriptome wide coverage of the AHBA microarray probes was used. Terms were considered to be significantly enriched if they showed a fold enrichment >1.0 and FDR-corrected $p < 0.05$, where fold enrichment was defined as the percentage of the differentially expressed genes belonging to that term, divided by the corresponding percentage in the background.

The PheWeb database includes genome-wide associations for 1403 EHR-derived ICD billing codes from 408,908 White British participants of the UK Biobank (Gagliano Taliun et al., 2020). According to the repository *"All individuals were imputed using the Haplotype Reference Consortium panel, resulting in >20 million variants. Analyses on binary outcomes were conducted using SAIGE (a generalized mixed model association test that uses the saddlepoint approximation to account for case-control imbalance), adjusting for genetic relatedness, sex, birth year and the first 4 principal components."* (Gagliano Taliun et al., 2020) Enrichment analysis in the PheWeb database (using the genes nearest to the disease-associated loci) was performed using the webinterface of Enrichr (Chen et al., 2013; Kuleshov et al., 2016; Xie et al., 2021), with as input the 223 differentially higher expressed genes. Disease term genetic associations were considered to be significantly enriched if they showed an odds ratio >1.0 and FDR-corrected $p < 0.05$, where the odds ratio was defined as the ratio of the proportion of a disease term in the differentially expressed genes list to the proportion of this disease term in all background genes (transcriptome wide protein coding genes).

We used a hypergeometric test to test for enrichment of gene sets defined as differentially expressed in psychiatric diseases according to two recent transcriptomic signature studies (Gandal et al., 2018; Girgenti et al., 2021). Data was extracted from DataTable S1 of the Gandal study (Gandal et al., 2018), and from the Supplementary Tables 1 and 22 of the Girgenty study (Girgenti et al., 2021). Genes were included in a disease group if they had an FDR-corrected p-value≤0.05 for the defined disease, and were divided into 'higher' or 'lower' differentially expressed according to having a log fold change higher than 0.1 or lower than −0.1 respectively. More stringent criteria resulted in empty gene groups. Inclusion of genes and categories of diseases according to both studies are summarized in Table S5.

For protein-protein interaction enrichment analysis and densely connected network discovery, the web-based tool Metascape (Zhou et al., 2019) was used, inputting the list of 223 differentially higher expressed genes that showed FDR-corrected $p < 0.05$. Metascape plots a graph of the inputted list of genes, where each node in the network is a protein encoded by one gene. Each edge represents a known physical interaction between the two proteins, where 'physical interaction' means two proteins are biochemically bound, either directly or through a complex. The resulting network plot visually represents known physical interactions between the proteins of interest. Within the resulting network, "densely connected" subnetworks are detected by the Molecular Complex Detection (MCODE) algorithm (Bader and Hogue, 2003). Densely connected subnetworks are defined as parts of the main network where each node (protein) has known physical interactions with all of the other nodes (proteins) in that network. Metascape uses the following databases for protein-protein interaction analysis: STRING, BioGrid, OmniPath and InWeb_IM. For the String and BioGrid database, only

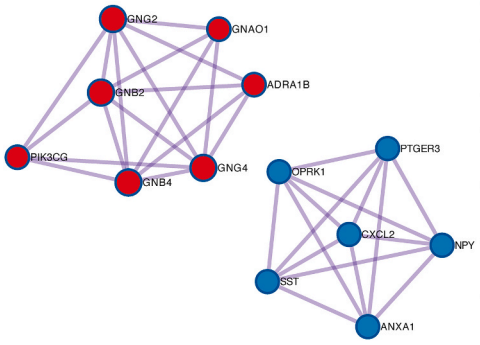

Color	MCODE	GO	Description	Log10(P)
	MCODE_1	R-HSA-392451	G beta:gamma signalling through PI3Kgamma	-14.3
	MCODE_1	hsa04725	Cholinergic synapse	-13.8
	MCODE_1	R-HSA-397795	G-protein beta:gamma signalling	-13.7
	MCODE_2	R-HSA-418594	G alpha (i) signalling events	-11.9
	MCODE_2	R-HSA-373076	Class A/1 (Rhodopsin-like receptors)	-11.7
	MCODE_2	R-HSA-500792	GPCR ligand binding	-10.9

Fig. 4. Densely connected networks of protein-protein interactions and their enrichment categories.GPCR: G protein-coupled receptor.

physical interactions were included (as these databases normally also include 'interactions' between proteins other than solely based on biochemical bonding, such as regulatory interactions derived from computational analyses – as these interactions are possibly less accurate, we only kept physical interactions). Subsequent pathway and process enrichment analysis (using hypergeometric tests) was performed on the densely connected subnetworks, including terms from the KEGG Pathway, GO Biological Processes, Reactome Gene Sets, Canonical Pathways, CORUM, WikiPathways and PANTHER Pathway databases (Zhou et al., 2019). Significantly enriched pathways and processes were defined as showing fold enrichment >1.5 with a p-value <0.01, where fold enrichment is the ratio between the observed counts and the counts expected by chance. Log10 transformations of p-values were used in the plot (Fig. 4).

Step 7. Cell enrichment analysis

To translate our results from the individual gene level to a cell type level that is verified in human, we performed cell type enrichment analysis using three datasets: 1) WebCSEA data including only human cell types (Dai et al., 2022), 2) Allen Cell Type Atlas data, including highly specific characterizations of human cortical neuronal cell subtypes (Hodge et al., 2019), 3) NeuroExpresso data including only brain cell types (Mancarci et al., 2017).

WebCSEA provides a web-based application for cell-type-specific enrichment analysis of genes, based on scRNA-seq panels of human tissues. Inputting our list of higher differentially expressed genes in the web-based interface, cell-type specificity was assessed across 1355 human tissue cell types. Although this method is good for assessing tissue specificity and general cell type specificity, the tool is not optimal for distinguishing between the many different inhibitory and excitatory subtypes of interneurons that were shown to exist across the human cortex (Hodge et al., 2019; Tasic et al., 2018).

That is why we additionally used the Allen Cell Type data measured in samples from human cortical areas (from the middle temporal gyrus), using single nucleus RNA sequencing followed by cortical neuronal cell type classification (Hodge et al., 2019). This dataset consists of a classification of 75 different GABAergic and glutamatergic cortical neuronal cell types, as well as cortical astrocytes and microglia. For enrichment analysis, we first concatenated the marker genes for each of these specific cell types as listed in Supplementary Table 2 of the paper by Hodge et al. (2019). Next, we used an inclusion threshold of having at least five different marker genes per cell type, which excluded five cell types (three inhibitory, and two excitatory neuronal cell types: Inh L2-5 VIP SERPINF1, Inh L4-6 SST B3GAT2, Inh L4-5 SST STK32A, Exc L5-6 THEMIS C1QL3, Exc L6 FEZF2 OR2T8). We then used a hypergeometric test to test for any significant overrepresentations ('enrichments') of cell type marker genes in our set of differentially expressed genes, using a threshold of $p < 0.05$ after Bonferroni correction, using the transcriptome wide coverage of the AHBA microarray probes as background.

For a very small selection of genes, it was found that, as far as cortical neuronal cell types are concerned, some genes have measurable expression only in one specific cell type (Hodge et al., 2019). Because our differential expression results are based on cortical tissue only, any of those 'cell-type-exclusive-genes' present in our results, might indicate enrichment of the related cell types – even if the hypergeometric test fails to reach significance, because of missing differential expression of other less specific marker genes. That is why we additionally cross-referenced our differentially expressed gene set for cell types that, according to the cortical cell type data – besides having multiple marker genes – showed single genes to be expressed highly specifically in that cell type.

Additionally, we used the NeuroExpresso (Mancarci et al., 2017) database to perform a similar cell type enrichment analysis for the higher differentially expressed genes. Genes were converted from rat to human orthologues using the "homologene" package in R, which is a wrapper for the Homologene database by the National Center for Biotechnology Information (NCBI) (Mancarcı, n.d.). Although rodent-derived and not specific for cortical neuronal cell types, this dataset contains more abundant putative marker genes for 20 other brain cell types, like microglia, oligodendrocytes and astrocytes. The number of included marker genes for each cell type are listed in Table S6. Threshold for calling "enrichment" of cell type (i.e. marker genes) significant was based on marker genes showing enrichment in the differential expression results using a threshold of $p < 0.05$ after Bonferroni correction, using the transcriptome wide coverage of the AHBA microarray probes as background.

To plot mean gene expression levels in human cortical cell types of the genes included in the densely connected networks discovered in the protein-protein interaction enrichment analysis (see above, *step 6*), we used recently added single nucleus RNA sequencing data, sampled from several locations of human cortical donor brains (middle temporal gyrus, anterior cingulate cortex, primary visual cortex, primary motor cortex, primary somatosensory cortex, primary auditory cortex), available at the Allen Cell Type atlas website (Allen Institute, 2019). These data list trimmed mean expression for each gene per distinguished cell type (Allen Brain Map, 2019). This dataset distinguishes a total of 120 different human cortical cell types. Trimmed means are calculated by first log2 transforming gene expression and then calculating the average expression of the middle 50% of the data (data with lowest and highest 25% of expression values removed) independently for each gene and cell type.

3. Results

3.1. Differential expression analysis

In order to analyze what defines cortisol rhythm sensitive cortical brain regions on a transcriptomic level, we performed differential gene

Table 1
Overview of samples from the six AHBA donors in the differentially GC-rhythm responsive area and the control regions.

	Donor	Donor	Donor	Donor	Donor	Donor	All
Differentially responsive area	10021	12876	14380	15496	15697	9861	donors
	6	10	10	13	8	14	61
Control region							
	169	168	249	209	222	207	1224

expression analysis using our fMRI data in combination with a high resolution transcriptomic human brain atlas. The brain regions that showed significant variations in the BOLD signal responses to emotional stimulation (exposure to emotionally valenced faces) between the pulsatile and the non-pulsatile group were matched with brain coordinates of the AHBA samples from the left cortex, as depicted in Fig. 1 (see Methods section for details). Note that although lateralization in function is well described, it has been established in multiple studies that there are no statistically significant transcriptional hemispheric differences in adult brain (Hawrylycz et al., 2012; Johnson et al., 2009). This indicates that post-transcriptional factors constitute hemispheric differences in function, while left and right hemispheres are similar on a gene transcription level. Because only two donor brains have been sampled bilaterally, while all six donor brains include samples from the left hemisphere, we maximized spatial resolution by mapping the fMRI effects of the right hemisphere to cortical AHBA sample coordinates of the left hemisphere by inverting the x-axis coordinates in MNI-152 space (Fig. 1A).

After selection of cortical samples, based on their inclusion in the cortical Desikan parcellation atlas (Desikan et al., 2006), 61 left cortical samples were mapped to the differentially responsive brain areas (regions corresponding to either “mask A” or “mask B″ in Figs. 1A), and 1224 left cortical samples were selected as control samples (Fig. 1B and Table 1).

Despite the gene expression normalization procedures performed by the AHBA (“Allen Human Brain Atlas,” 2013), it has been established that large inter-individual differences in gene expression remain in the AHBA samples (Arnatkeviciute et al., 2019). We too find that for the 1285 left cortical samples used in our differential expression analysis, samples from the same brain have more similar gene expression levels (Fig. 1C). To account for these between-donor effects, and additionally any between-sample effects in our differential expression analysis, we applied both within-sample and across-sample normalization strategies (see Methods section) (Arnatkeviciute et al., 2019). We visualize the efficacy of these strategies by running a t-distributed Stochastic Neighbor Embedding (tSNE) on all 1285 included cortical samples before and after preprocessing steps (Fig. 1C).

After all preprocessing steps and probe selection criteria were applied, differential expression analysis was performed for 10014 gene transcripts, comparing 61 AHBA samples (cases) with 1224 AHBA samples (controls). This resulted in 304 genes that showed significant differential expression after correcting for false discovery rate (FDR), with the significancy threshold set at Benjamini-Hochberg corrected $p < 0.05$. 223 genes showed a differentially higher expression, and 81 genes showed a differentially lower expression. The top 25 of differentially expressed genes are plotted in Fig. 2A (for a full list see Table S2).

Although possible donor-driven effects were mitigated by extensive normalization strategies, we additionally tested the possibility of incomparable transcriptomic signatures between donor brains (for example due to age, gender, ethnicity etc.) that might invalidate the differential expression analysis. We did this by using the differential stability (DS) metric: a correlation-based measure for the consistency of a gene’s differential expression pattern across brain structures (Shaw et al., 2011). We used the fact that gene expression patterning across brain structures was assessed for reproducibility in all six AHBA donor brains in previous works (Hawrylycz et al., 2015; Quintana et al., 2019). By cross-referencing our differentially expressed genes list with these previous results (Supplementary Table 2 of the study by Hawrylycz et al. (2015)), we find that our differentially expressed genes show high median differential stability in comparison to other genes (median = 0.74 versus median = 0.53, $p < 0.001$). This indicates that the identified genes have reproducible gene expression patterns across all donor brains, regardless of sex, age and other donor related factors (Fig. 2B).

3.2. *Differential gene expression in pulsatility-sensitive brain regions shows neuronal specificity and enrichment for retrograde endocannabinoid signaling*

In order to establish whether the differential expression results were specific to brain cell expression patterns, and to interpret the differential expression results in terms of biological pathways and processes, we analyzed the differentially expressed genes for enrichment of gene ontology (GO) terms (including GO terms relating to cellular components, biological processes, and molecular functions) and Kyoto Encyclopedia of Genes and Genomes (KEGG) pathway categories (Fig. 3). Using all 223 genes that showed higher differential expression in the pulsatility-responsive brain regions, we found significant enrichment for 37 different GO terms related to cellular components and biological processes (FDR corrected $p < 0.05$, see Table S3). Most notably, terms relating to neurons (e.g. neuron part, neuron development, neuron projection) and intercellular communication (e.g. signaling, cell communication, synapse, response to stimulus) were found to be enriched, confirming neuronal specificity of differential gene expression in pulsatility-responsive brain regions. Significant enrichment for KEGG pathways (FDR corrected $p < 0.05$) was found for the categories ‘retrograde endocannabinoid signaling’, ‘glutamatergic synapse’, ‘GABAergic synapse’ and ‘morphine addiction’ (see Fig. 3 and Table S3). In the 81 genes with lower differential expression, none of the positive hits in the GO term enrichment analysis showed statistically significance after FDR correction (Table S4). Enrichment analysis for KEGG pathways in these 81 genes yielded one positive hit but reached no statistically significance (Table S4).

3.3. *Differentially expressed genes in pulsatility-sensitive cortical brain regions show enrichment for transcriptomic signatures of stress-related psychiatric disease*

To further relate the transcriptomic signature of the rhythm-sensitive brain regions to possible disease mechanisms, we tested for enrichment of brain gene expression patterns of several psychiatric disorders in our differentially expressed genes. Using two recent brain transcriptomic studies defining brain transcriptomic signatures for several psychiatric disorders based on several tissue types (Gandal et al., 2018; Girgenti et al., 2021), we tested for enrichment of our higher and lower differentially expressed genes in these transcriptomic signatures (see Table S5 for all results). In one study including both MDD and PTSD brain samples (Girgenti et al., 2021), we found enrichment of both MDD and PTSD genes in our 223 higher differentially expressed genes (Table S5). Using a second study including multiple psychiatric diseases (Gandal et al., 2018), our differentially higher expressed genes were enriched for genes showing higher differential expression in autism spectrum disorder (ASD), bipolar disorder (BD) and alcoholic abuse disorder (AAD). In our 81 differentially lower expressed genes, we found enrichment for genes showing differentially lower expression in ASD, schizophrenia (SCZ) and

BD (Table S5). In further validation of our differential expression results in relation to stress-related disorders, we performed additional enrichment analysis using the PheWeb database: a dataset based on genome-wide associations for EHR-derived diagnoses in the UK Biobank (Gagliano Taliun et al., 2020). We found the most enriched category (meaning having the highest odds ratio and lowest p-value) to be 'Acute reaction to stress' (odds ratio = 24.50, corrected p = 0.099), although the FDR-corrected p-value did not reach the threshold of significance (see Fig. S1).

3.4. Protein-protein interaction enrichment analysis reveals association of pulsatility-responsive brain regions with particular $G_i\alpha$ signaling events

To interpret our differential expression results on a functional protein level, we analyzed proteins encoded by the differentially expressed gens for known protein interaction networks related to specific biological pathways. Using the list of 223 differentially expressed genes that show higher expression in the pulsatility-responsive brain regions, protein-protein interaction enrichment of the proteins encoded by those genes was analyzed using multiple databases (see Methods section) to plot a network containing all proteins (encoded by our differentially expressed gene list) that have documented interactions with at least one other protein in the list (Fig. S3). Next, using the MCODE algorithm (Bader and Hogue, 2003) for detection of densely connected network components within this network, we found two densely connected networks in the main network, and one separate densely connected network consisting of only three gene products (SOX5, ZFP36, MAGED1) (Fig. S3). Subsequent pathway and process enrichment analysis for each of these three densely connected networks only yielded significant enrichment hits for the two subnetworks contained in the main interaction network (colored red and blue in Fig. S3). One subnetwork consisted of ADRA1B, GNAO1, GNG2, GNG4, GNB2, GNB4 and PIK3CG, and showed enrichment for G-potein beta-gamma signaling through PIK3Kgamma ($p = 5.01e^{-15}$), more generic G-protein beta-gamma signaling ($p = 2.00e\text{-}^{14}$) and cholinergic synapse ($p = 1.58e^{-14}$) (Fig. 4). The other densely connected network consisted of protein-protein interactions between NPY, ANXA1, SST, PTGER3, OPRK1 and CXCL2, and showed enrichment for $G\alpha_i$ signaling events ($p = 1.26e^{-12}$), and (more generic) G protein-coupled receptor (GPCR) ligand binding ($p = 1.26e^{-11}$), as well as a subclass of GPCRs, the rhodopsin-like receptors ($p = 2.00e^{-12}$). These results further support the notion that GC rhythm alterations act directly on the brain and will have most effect in brain regions that, on an anatomical transcriptional patterning level, show to be enriched for genes related to particular GPCR functionality. The same analysis performed on the set of genes with lower differential expression did not result in any densely connected networks showing significant enrichment.

3.5. Cortical cell type analysis reveals exclusive enrichment of GABAergic neurons and differentially expressed genes specific to certain cell types

To further investigate cortical patterning related to rhythm sensitivity on a cell type level, we analyzed whether the found transcriptomic signature showed enrichment of marker genes of several brain cell types, including data on highly detailed subtyping of inhibitory and excitatory interneurons.

Using the WebCSEA interface, inputting our 223 higher differentially expressed genes showed brain tissue specificity, as well as cell type specificity for neuronal cell types (both excitatory and inhibitory neurons) (Fig. S2). To further specify distinguished neuronal subtypes, we used the 223 higher differentially expressed genes for cell type enrichment analysis using marker gene data on 75 human cortical cell subtypes (see Methods section (Hodge et al., 2019),). Using this data, enrichment analysis showed an exclusive enrichment of marker genes of GABAergic cell types. Specifically, the three cell types found to show enrichment of their respective marker genes in our differential expression results were the GABAergic SP8-expressing interneurons (belonging to a cluster of neurons expressing PAX6 and TNFAIP8L3); EGFEM1P-expressing interneurons (belonging to the cluster of neurons expressing VIP and PENK); and the QRFPR-expressing interneurons (belonging to the cluster of neurons expressing SST and GXYLT2) (Fig. 5). Using the 81 lower differentially expressed genes showed no enrichment for any of the neuronal cell types (Fig. 5).

For the 223 higher differentially expressed genes, cross-referencing of single marker genes, specific and sufficient for the classification of a single cortical neuronal cell type (see Methods section), yielded a match with one specific GABAergic NPY-expressing interneuron. When taking all marker genes for this cell type into account, the NPY-expressing interneurons failed to reach significance in our hypergeometric enrichment analysis, as not all marker genes were present in our differentially higher expressed gene set. However, in the cell type dataset, NPY gene expression was found to be highly specific for a single inhibitory cell type (Fig. S2) (Hodge et al., 2019). Even though the NPY-expressing neuronal cell type failed to reach significance in the hypergeometric test ($p = 0.265$), we thus consider the significantly higher expression of NPY in the examined brain regions an indication of an enrichment of the specific NPY-expressing GABAergic neurons in those regions.

To further look on a cell type level at the MCODE component genes in the protein-protein interaction analysis – which also contains NPY – we used the gene expression levels by cell type from a recently added single nucleus RNA sequencing cluster-based cell type dataset, consisting of 120 distinguished human cortical cell types (see Methods section) (Allen Brain Map, 2019). The results are plotted in Fig. 6, and again show a specific GABAergic neuronal cell type ("Inh L6 SST NPY") that shows highly specific expression of the NPY gene. The same plot including the top-50 higher differentially expressed genes and both cortisol receptors (GR and MR) is shown as Fig. S4.

In addition to the specific human cortical neuronal cell type datasets, that include a vast majority of cortical neuronal cell types, we also

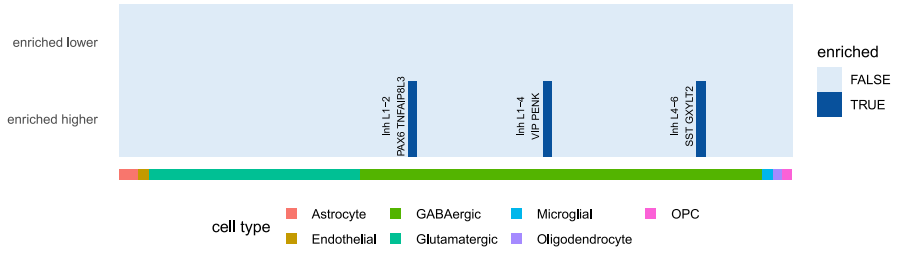

Fig. 5. Results of human cortical cell type enrichment analysis reveal four inhibitory neuronal cell types for the differentially higher expressed genes (DEG higher). For the lower expressed genes (DEG lower) no neuronal cell types were found to be enriched. Results of NeuroExpresso cell type data enrichment analysis are included as extended data in Table S6.

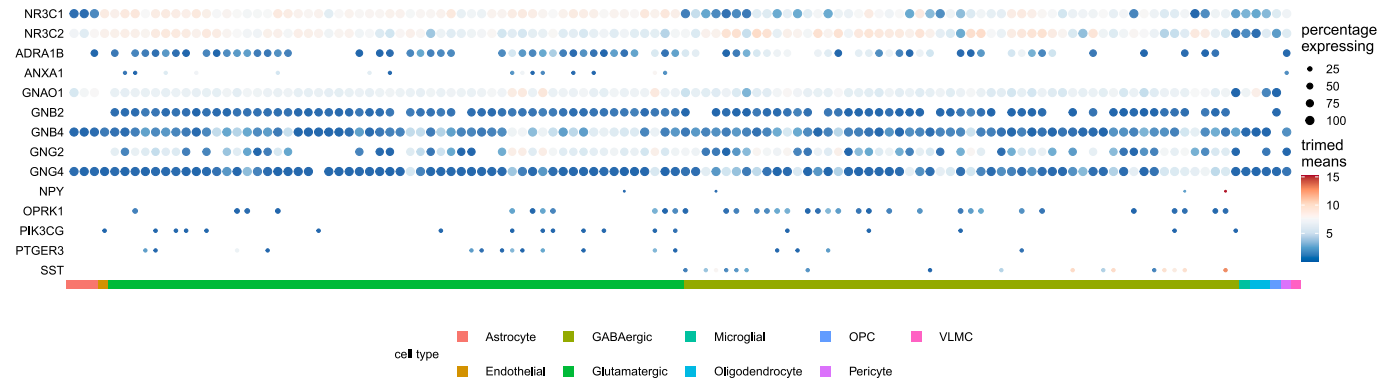

Fig. 6. Dot plot of trimmed mean gene expression per cell type for GR, MR, and the identified MCODE cluster, and their specificity (percentage of cell types expressing them). Genes with a trimmed mean expression of 0 in all cell types (meaning they show expression in less than 25% of cells for each cell type) are omitted from the plot (see Methods section for details). The red arrow points to high mean expression (dark red colored dot) of NPY very specific for a particular SST-expressing GABAergic neuronal cell type. The same plot for the top-50 of differentially expressed genes is included in the extended data as Fig. S2. (For interpretation of the references to color in this figure legend, the reader is referred to the Web version of this article.)

looked at enrichment in a larger cross-laboratory, rodent-derived dataset containing putative marker genes for different cell types in the brain, not specific to either cortical regions or neuronal subpopulations (Mancarci et al., 2017). We found a significant enrichment for marker genes of microglia, Purkinje cells and serotonergic cells (Table S6).

4. Discussion

In this study we investigate the transcriptional and cell type patterning of brain regions that are sensitive to cortisol pulsatility. Strikingly, both the top significant differentially expressed gene (ANXA1) and the most significantly enriched KEGG pathway term (retrograde endocannabinoid signaling) have been identified before as key components of rapid non-genomic GC signaling (Atsak et al., 2012; Di et al., 2016; Tasker and Herman, 2011; Tierney et al., 2003).

The endocannabinoid system has emerged as an important regulator of some of the rapid, non-genomic glucocorticoid effects in the brain (Atsak et al., 2012; Di et al., 2016; Tasker and Herman, 2011). The mechanism involves the glucocorticoid-mediated activation of membrane associated variants of the GRs at the target brain cells (mainly postsynaptic sites) to induce endocannabinoid synthesis and/or local release, causing retrograde cannabinoid type I receptor-mediated modulation of the presynaptic neuronal activity. This mechanism has been described as responsible for (i) the hormonal negative feedback regulation of excitatory synaptic inputs to hypothalamic (paraventricular nucleus) neuroendocrine cells (Tasker and Herman, 2011), and (ii) the long-lasting suppression of spontaneous inhibitory synaptic inputs (Di et al., 2016) as well as facilitation of excitatory inputs to the basolateral amygdala principal neurons induced by glucocorticoids in the acute stress setting (Karst et al., 2010), while (iii) a similar involvement of this glucocorticoid-induced mechanism has been also described for the attenuation of inhibitory transmission in prelimbic cortex, again under stressful conditions (McReynolds et al., 2018). Our data suggest that cortical brain regions with the capacity of recruiting the retrograde endocannabinoid signaling pathway may be more sensitive to the characteristics of the ultradian glucocorticoid rhythm, i.e., able to convert changes in glucocorticoid pulsatility into different neurobiological effects (in our case differential neural activation in response to the same emotional stimuli).

The ANXA1 finding is also of great interest as it has been implicated as a facilitator in the rapid non-genomic inhibitory feedback effects of endogenous glucocorticoids on ACTH release (Tierney et al., 2003). Although these findings were limited to the folliculo-stellate cells in the anterior pituitary gland, the ANXA1 gene has also been implicated in the neuroprotective and anti-inflammatory role of microglia (McArthur et al., 2010). Although sparse ANXA1 gene expression has been demonstrated in microglia of human brains (McArthur et al., 2010), the extensive cortical cell type data based on single nucleus RNA sequencing of multiple cortical regions of the human brain (Allen Brain Map, 2019; Allen Institute, 2019) that we used here, shows ANXA1 gene expression to be mostly apparent in excitatory neuronal cells (Fig. S4). In this data, ANXA1 does not show any pronounced expression (trimmed means > 0) in the microglial cell types of the human cortical cell type data (Fig. S4). ANXA1 is however listed as a microglial marker gene in the Neuro-Expresso rodent-based data.

ANXA1 is also part of the defined densely connected network of protein-protein interactions that drives enrichment of terms related to GPCR function, more specifically $G\alpha_i$ signaling events. This enrichment can be interpreted as an indication of i) the involvement of a specific (set of) cortisol activated GPCR(s) associated with G alpha i proteins, ii) membrane GR/MR having a hitherto unknown association with $G\alpha_i$ signaling events, iii) cross-talk between GR/MR signaling and signaling cascades involving these G protein species. For example, this could mean that a cortisol pulse is linked to an inhibitory transmission effect ($G\alpha_i$) (Neves et al., 2002). Additionally, the interaction network showed enrichment of G-protein beta and gamma subunits and linked this to acetylcholine receptor signaling. It was previously demonstrated that intracellular calcium signaling via the mAChR3 subtype depends on the beta 2, gamma2 and gamma 4 subunits that are present in the MCODE-1 network (Khan et al., 2015). This suggests a link between calcium regulation and the sensitivity to cortisol pulses, perhaps involving annexin A1 (Lim and Pervaiz, 2007).

Our WebCSEA results reiterate the GO-analysis results, again showing neuronal cell type specificity of the differentially expressed genes (with hits for both inhibitory and excitatory neurons). The results of our specific cortical cell subtype analysis, using more detailed gene expression profiling of subtypes of both excitatory and inhibitory neuronal subtypes, show exclusive enrichment for GABAergic neurons. This is of interest because evidence has consistently implicated (SST expressing) GABAergic interneuron dysfunction in MDD (Major Depressive Disorder) pathology (Levinson et al., 2010; Luscher et al., 2011). Additionally, differential higher expression of NPY in our brain region of interest might indicate 'enrichment', or relative abundance, of a specific SST-NPY expressing GABAergic interneuron. Although NPY seems to be highly selectively expressed by one cortical neuronal subtype, it should be noted that NPY is also expressed in subcortical

neurons, and not specific to neuronal cell types only (Carniglia et al., 2017).

Both hypercortisolemia and circadian rhythm alterations have been related to MDD subtypes and MDD pathology in general (Keller et al., 2017). Our results additionally seem to point to the importance of ultradian rhythm disturbances in the process of GABAergic interneuron dysfunction in MDD pathology. In our differentially expressed genes, we did in fact find enrichment of an MDD brain transcriptomic signature as defined by one recent study (Girgenti et al., 2021). However, we did not find an MDD brain transcriptomic signature enrichment when using the transcriptomic signature defined by another study (Gandal et al., 2018).

Although anatomical cell type enrichment in our defined brain regions appears to be exclusive for GABAergic neurons in the human cortical cell type data, inspection of the cell type specific expression shows excitatory neuron specificity for some differentially expressed genes as well. Specifically, ANXA1 and NR4A2 show expression predominantly in glutamatergic neuronal cell types (see Fig. S4). This implies that, although there might be an important role for GABAergic signaling in pulsatility sensitivity, the $G\alpha_i$ and $G\alpha_q$ signaling events implicated in the differential brain activational response to cortisol rhythm changes are not specific to GABAergic cell types but occur in glutamatergic neurons as well.

No microglial enrichment was found in the human cortical cell type analysis, but it was found in NeuroExpresso-based results. The enrichment analysis using the NeuroExpresso data, however, is more difficult to interpret, as the marker gene data used here are rodent derived, not cortex specific and therefore not comparable to the standard of tissue processing and measuring protocols from the human cell type data (i.e. mainly microarray based, different labs with different procedures were used) (Allen Brain Map, 2019). Also, while only six marker genes were included for microglial cells in the human cortical cell type data (Hodge et al., 2019), the NeuroExpresso datasets lists over a hundred unique marker genes for microglia (see Table S6). Depending on the specificity of those genes, an abundance of marker genes could lead to an increase in false positive results. Yet, there is considerable evidence for a role of microglia in the stress response and transcriptomic dysregulation of microglia, although mostly in the context of overactivation in chronic stress (Réus et al., 2015; Wohleb, 2016).

4.1. Limitations and strengths

It is important to note that we only describe anatomical transcriptomic patterns, based on healthy donor brains, and do not investigate putative brain transcriptional effects in the brains of the participants of the pulsatility study. The aim of our current study was to investigate the anatomical transcriptional and cell type patterning of pulsatility sensitive brain regions. Notably, this is unrelated to any local transcriptional effects that loss of ultradian cortisol rhythm might have on specific brain regions, and does not include any post-transcriptional factors that can explain observed lateralization in function.

The AHBA provides the most detailed dataset for examining spatial distribution of human brain transcriptomics to date but is limited to six donor brains. Another differential expression analysis with the same spatial resolution would not be possible in other publicly available data at this time. Importantly, it should be noted that to mitigate any donor-driven bias, and to control for any possible incomparability of gene expression levels due to donor-specific differences (e.g. age, gender, ethnicity) we 1) did thoroughly correct for any donor-driven gene expression bias, 2) used a regression based method that allows for repeated sampling from the same subjects, and 3) checked the comparability of gene expression patterning of differentially expressed genes across donor brains using the differential stability criterion. The outcome of these control measurements (see Figs. 1C and 2B) indicate an unbiased differential expression analysis and reproducible results across all 6 donor brains, regardless of demographic or biological differences of donors. Although we estimate the sample size (i.e. $n = 1285$) coming from these six donors to be sufficient for the scope of our current analyses, including more donor brains with the same spatial resolution likely would have further improved the generalizability of the current results to brains with a more substantial diversity of donor characteristics.

It deserves mentioning that our analysis uses unbalanced groups, as we compared 61 brain samples versus 1224 other brain samples. This is important to be recognized, as imbalanced data can result in reduced statistical power (Lydersen, 2018; van Belle, 2008a). However, using a substantially larger set of 'control samples' (1224 brain samples) than 'case samples' (61 brain samples) can substantially increase statistical power compared to a scenario where 61 'case samples' would have been compared to '61 control samples' (Lydersen, 2018). Although an increased number of controls increases statistical power, it has been suggested that as a rule of thumb, increasing the largest group to more than five times the smallest group, might not result in significant further increase of statistical power (van Belle, 2008b). In terms of statistical power, then, using 1224 control samples might not be better than using 300 control samples. Biologically, however, it is needed to include all control samples, as we aim to investigate the transcriptional landmark of the brain areas affected by cortisol pulsatility compared to the rest of the cortex that did not seem to be affected in the same way.

We define a cortical brain region as 'pulsatility sensitive', i.e. showing a differential pattern of neural activation between physiological pulsatile and non-pulsatile groups, on the basis of a task-based fMRI study. It is therefore possible that additional cortical regions could be defined as 'pulsatility sensitive' in a different task-based setting. Our results thus formally define transcriptional and cell type patterns of regions that are pulsatility sensitive in the context of emotional processing. Accordingly, we selected 'rest-of-cortex' as control samples in our differential expression analysis because the fMRI results are based on a whole-brain analysis - in the context of emotional processing. Importantly, these fMRI results reflect significant differences in neural activation during emotional processing between both groups (see Supplementary Fig. S4 of Kalafatakis et al. (2018). This means that the statistical maps we used in our analysis are unrelated and independent to mean task activation (i.e., a brain region might show a distinct mean neural response to the task, but might not at all show differential fluctuation of activation during task conditions between groups, and vice versa). Consequently, it would be invalid to select 'control samples' only from regions showing significant base neural response to the task. To illustrate, we thresholded a separately calculated statistical map for mean task activation to exactly include all significantly differential responsive regions (meaning that the significantly differential responsive region with the lowest mean task activation is used as a threshold for "task activation"). Using this threshold, virtually the whole brain can be defined as 'activated by task'. For these reasons, we chose to use "rest-of-cortex" as control samples.

The task-based setting used in our fMRI study, with a validated paradigm for probing emotional processing, has several advantages. First, we found differences in emotional processing on a functional level between pulsatility groups, meaning that the imaging effects correlate to functional effects as well (Kalafatakis et al., 2018). Second, by using the context of emotional processing, effects of loss of ultradian rhythm are likely related to brain functionality affected by cortisol signaling related pathologies such as major depressive disorder, posttraumatic stress disorder and other stress related psychiatric disorders.

In fact, we did find enrichment of differentially expressed genes related to transcriptomic brain signatures described in both PTSD and MDD, but also ASD, BD, SCZ and AAD. A difficulty with interpreting these enrichment results is that defined differentially expressed gene sets in both transcriptomic studies used for gene set definition (Gandal et al., 2018; Girgenti et al., 2021) are based on several brain tissues from non-overlapping anatomical origins. None of the tissues included in these studies overlaps with the fMRI mask we used for our differential expression analysis. In this regard it is also important to note that even

the same neuronal cell type can have a different transcriptomic profile depending on the cortical region it is embedded in, indicating the possible loss of power using several different non-overlapping tissues (Beerens et al., 2022). Another issue is that MDD enrichment was found when using one study by Girgenti et al. (2021), but not when using the MDD gene set as defined by the study by Gandal et al. (2018). This further indicates the difficulty of comparing different brain tissues, especially given a lack of robust marker genes throughout tissue types (which was the case for the data by Girgenti et al.). Although the study by Gandal et al. lists correlated log2 fold change in differentially expressed genes across disorders, and results from this study that are shared amongst different brain areas and diseases might be more robust, there is only one gene that satisfies the condition of having an FDR-corrected p-value <0.05 in all five disorders (gene: CRH). This might explain the lack of enrichment of our differential expression results for the 'all-diseases' group of genes as defined by the Gandal study.

It deserves further mentioning that the disease-enrichment analysis using the PheWeb dataset (Gagliano Taliun et al., 2020), which listed "Acute reaction to stresss" as a top enriched term (odds ratio = 24.50, FDR-corrected $p = 0.099$), neither reached threshold significance (which we defined as $q < 0.05$), nor was based on a highly specific dataset. The PheWeb data was collected as part of the UK Biobank, that uses data from regular care sources. Specific brain diseases might not be as commonly diagnosed as bladder infections or types of cancer (Fig. S1). In all this aspecificity, it is interesting to see "Acute reaction to stress" come up as a first hit nonetheless, although one can question its reliability for the reasons mentioned above.

Cell type enrichment analysis was based on human cortical cell type data, which we consider a strength of the study. However, as these data distinguishes more inhibitory than excitatory neuronal cell types, and lists approximately twice as many combined inhibitory marker genes than excitatory marker genes (386 versus 173), there is a possible bias towards inhibitory cell enrichment. The significantly higher expression of the NPY gene – which is highly specific for a specific SST expressing cluster of inhibitory neuronal cell types – and the fact that the differentially expressed genes show enrichment for four inhibitory cell types, but no excitatory cell types, do seem to point to the importance of a GABAergic neuronal response to cortisol pulsatility.

As discussed in relation to microglia, the additional cell type enrichment analysis using NeuroExpresso cell type data might not reflect optimal marker gene specificity. For some enriched cell types, NeuroExpresso marker genes also seem to be non-specific upon further inspection (Table S6). For example, the enrichment found for 'serotonergic cells' is based on the inclusion of two genes (TRH and PTGER3), that are in fact not specific for serotonergic cells. Obviously, serotonin producing cell bodies should be absent or very scarce in cortical cells. Assuming that these markers are not abundant in axonal projections of 5-HT neurons, and given that these 'marker' genes are not exclusive for 5-HT neurons, we consider this enrichment call to be a false positive outcome.

The aim of this study was to investigate the anatomical transcriptional and cell type patterning of pulsatility sensitive brain regions. We show that the loss of cortisol ultradian rhythmicity alters emotional processing response in cortical brain areas that are characterized by transcriptional and cellular profiles of GABAergic functioning. Our results indicate that specific cell types and G protein signaling cascades underly the cerebral effects of loss of physiological cortisol rhythm, thus making these cell types and cascades a target for manipulation in future experimental studies.

Overall, in this study, we have identified target genes, signaling pathways and neuronal subtypes that might constitute key players in the physiological response to glucocorticoid pulsatility and its translation to differential biological effects in the human brain.

CRediT authorship contribution statement

Philippe C. Habets: Conceptualization, Data curation, Formal analysis, Investigation, Methodology, Project administration, Resources, Software, Visualization, Writing – original draft, Writing – review & editing. **Konstantinos Kalafatakis:** Conceptualization, Data curation, Formal analysis, Investigation, Methodology, Resources, Writing – original draft, Writing – review & editing. **Oleh Dzyubachyk:** Data curation, Formal analysis, Methodology, Supervision, Validation, Writing – review & editing. **Steven J.A. van der Werff:** Data curation, Formal analysis, Methodology, Supervision, Validation, Writing – review & editing. **Arlin Keo:** Conceptualization, Data curation, Methodology, Supervision, Validation, Writing – review & editing. **Jamini Thakrar:** Data curation, Resources, Writing – review & editing. **Ahmed Mahfouz:** Conceptualization, Methodology, Resources, Supervision, Validation, Writing – review & editing. **Alberto M. Pereira:** Investigation, Resources, Writing – review & editing. **Georgina M. Russell:** Funding acquisition, Resources, Writing – review & editing. **Stafford L. Lightman:** Conceptualization, Funding acquisition, Investigation, Resources, Supervision, Validation, Writing – original draft, Writing – review & editing. **Onno C. Meijer:** Conceptualization, Investigation, Project administration, Resources, Supervision, Validation, Writing – original draft, Writing – review & editing.

Declaration of competing interest

The authors declare that they have no known competing financial interests or personal relationships that could have appeared to influence the work reported in this paper.

Data availability

All code used for the analyses is made available at https://github.com/pchabets/fMRI-transcriptomics-cortisol (also included in manuscript file).

Acknowledgments

Philippe Habets would like to express his gratitude to Aurina Arnatkevičiūtė for her support and guidance in the field of fMRI transcriptomics, the availability of the MATLAB pipeline for AHBA data, and to the highly insightful and useful work on combining AHBA and imaging data she and others of the Fornito lab have published. Konstantinos Kalafatakis would like to express his gratitude to Bodossaki Foundation (https://www.bodossaki.gr/en/) for supporting the research on modelling biomedical data, especially related to glucocorticoid biorhythmicity. The fMRI data was obtained from studies funded by the Medical Research Council and the Wellcome Trust to Stafford Lightman.

Appendix A. Supplementary data

Supplementary data to this article can be found online at https://doi.org/10.1016/j.ynstr.2023.100514.

References

Allen Institute, 2019. Allen Institute for brain science. Allen cell types database, 2019). Available at: https://celltypes.brain-map.org/rnaseq/human_ctx_smart-seq.

Allen Brain Map, 2019. Cell types database: human multiple cortical areas SMART-seq [WWW Document]. URL. https://portal.brain-map.org/atlases-and-data/rnaseq/human-multiple-cortical-areas-smart-seq.

Allen human brain atlas [WWW document]. URL. http://help.brain-map.org/display/humanbrain/Documentation.

Arloth, J., Bader, D.M., Röh, S., Altmann, A., 2015. Re-annotator: annotation pipeline for microarray probe sequences. PLoS One 10, e0139516.

Arnatkeviciute, A., Fulcher, B.D., Fornito, A., 2019. A practical guide to linking brain-wide gene expression and neuroimaging data. Neuroimage 189, 353–367. https://doi.org/10.1016/j.neuroimage.2019.01.011.

Atsak, P., Roozendaal, B., Campolongo, P., 2012. Role of the endocannabinoid system in regulating glucocorticoid effects on memory for emotional experiences. Neuroscience 204, 104–116. https://doi.org/10.1016/j.neuroscience.2011.08.047.

Bader, G.D., Hogue, C.W. v, 2003. An automated method for finding molecular complexes in large protein interaction networks. BMC Bioinf. 4, 2. https://doi.org/10.1186/1471-2105-4-2.

Bauduin, S.E.E.C., den Rooijen, I.L.B., Meijer, M., van der Werff, S.J.A., Keo, A., Dzyubachyk, O., Pereira, A.M., Giltay, E.J., van der Wee, N.J.A., Meijer, O.C., Mahfouz, A., 2021. Potential associations between immune signaling genes, deactivated microglia, and oligodendrocytes and cortical gray matter loss in patients with long-term remitted Cushing's disease. Psychoneuroendocrinology 132, 105334. https://doi.org/10.1016/j.psyneuen.2021.105334.

Beerens, S., Winterer, J., Lukacsovich, D., Földy, C., Wozny, C., 2022. Transcriptomically-guided pharmacological experiments in neocortical and hippocampal NPY-positive GABAergic interneurons. eNeuro 9. https://doi.org/10.1523/ENEURO.0005-22.2022. ENEURO.0005-22.2022.

Burt, J.B., Demirtaş, M., Eckner, W.J., Navejar, N.M., Ji, J.L., Martin, W.J., Bernacchia, A., Anticevic, A., Murray, J.D., 2018. Hierarchy of transcriptomic specialization across human cortex captured by structural neuroimaging topography. Nat. Neurosci. 21, 1251–1259. https://doi.org/10.1038/s41593-018-0195-0.

Carniglia, L., Ramírez, D., Durand, D., Saba, J., Turati, J., Caruso, C., Scimonelli, T.N., Lasaga, M., 2017. Neuropeptides and microglial activation in inflammation, pain, and neurodegenerative diseases. Mediat. Inflamm., 5048616 https://doi.org/10.1155/2017/5048616, 2017.

Chen, E.Y., Tan, C.M., Kou, Y., Duan, Q., Wang, Z., Meirelles, G.V., Clark, N.R., Ma'ayan, A., 2013. Enrichr: interactive and collaborative HTML5 gene list enrichment analysis tool. BMC Bioinf. 14, 128. https://doi.org/10.1186/1471-2105-14-128.

Dai, Y., Hu, R., Liu, A., Cho, K.S., Manuel, A.M., Li, X., Dong, X., Jia, P., Zhao, Z., 2022. WebCSEA: web-based cell-type-specific enrichment analysis of genes. Nucleic Acids Res. 50, W782–W790. https://doi.org/10.1093/nar/gkac392.

Desikan, R.S., Ségonne, F., Fischl, B., Quinn, B.T., Dickerson, B.C., Blacker, D., Buckner, R.L., Dale, A.M., Maguire, R.P., Hyman, B.T., Albert, M.S., Killiany, R.J., 2006. An automated labeling system for subdividing the human cerebral cortex on MRI scans into gyral based regions of interest. Neuroimage 31, 968–980. https://doi.org/10.1016/J.NEUROIMAGE.2006.01.021.

Di, S., Itoga, C.A., Fisher, M.O., Solomonow, J., Roltsch, E.A., Gilpin, N.W., Tasker, J.G., 2016. Acute stress suppresses synaptic inhibition and increases anxiety via endocannabinoid release in the basolateral amygdala. J. Neurosci. 36, 8461–8470. https://doi.org/10.1523/JNEUROSCI.2279-15.2016.

Fresno, C., Fernández, E.A., 2013. RDAVIDWebService: a versatile R interface to DAVID. Bioinformatics 29, 2810–2811. https://doi.org/10.1093/bioinformatics/btt487.

Fulcher, B.D., Little, M.A., Jones, N.S., 2013. Highly comparative time-series analysis: the empirical structure of time series and their methods. J. R. Soc. Interface 10, 20130048. https://doi.org/10.1098/rsif.2013.0048.

Gagliano Taliun, S.A., VandeHaar, P., Boughton, A.P., Welch, R.P., Taliun, D., Schmidt, E.M., Zhou, W., Nielsen, J.B., Willer, C.J., Lee, S., Fritsche, L.G., Boehnke, M., Abecasis, G.R., 2020. Exploring and visualizing large-scale genetic associations by using PheWeb. Nat. Genet. https://doi.org/10.1038/s41588-020-0622-5.

Gandal, M.J., Haney, J.R., Parikshak, N.N., Leppa, V., Ramaswami, G., Hartl, C., Schork, A.J., Appadurai, V., Buil, A., Werge, T.M., Liu, C., White, K.P., Horvath, S., Geschwind, D.H., 2018. Shared molecular neuropathology across major psychiatric disorders parallels polygenic overlap. Science 359, 693–697. https://doi.org/10.1126/science.aad6469.

Girgenti, M.J., Wang, J., Ji, D., Cruz, D.A., Stein, M.B., Gelernter, J., Young, K.A., Huber, B.R., Williamson, D.E., Friedman, M.J., Krystal, J.H., Zhao, H., Duman, R.S., 2021. Transcriptomic organization of the human brain in post-traumatic stress disorder. Nat. Neurosci. 24, 24–33. https://doi.org/10.1038/s41593-020-00748-7.

Habets, P.C., Mclain, C., Meijer, O.C., 2021. Brain areas affected by intranasal oxytocin show higher oxytocin receptor expression. Eur. J. Neurosci. 54, 6374–6381. https://doi.org/10.1111/ejn.15447.

Hawrylycz, M.J., Lein, E.S., Guillozet-Bongaarts, A.L., Shen, E.H., Ng, L., Miller, J.A., van de Lagemaat, L.N., Smith, K.A., Ebbert, A., Riley, Z.L., Abajian, C., Beckmann, C.F., Bernard, A., Bertagnolli, D., Boe, A.F., Cartagena, P.M., Chakravarty, M.M., Chapin, M., Chong, J., Dalley, R.A., Daly, B.D., Dang, C., Datta, S., Dee, N., Dolbeare, T.A., Faber, V., Feng, D., Fowler, D.R., Goldy, J., Gregor, B.W., Haradon, Z., Haynor, D.R., Hohmann, J.G., Horvath, S., Howard, R.E., Jeromin, A., Jochim, J.M., Kinnunen, M., Lau, C., Lazarz, E.T., Lee, C., Lemon, T.A., Li, L., Li, Y., Morris, J.A., Overly, C.C., Parker, P.D., Parry, S.E., Reding, M., Royall, J.J., Schulkin, J., Sequeira, P.A., Slaughterbeck, C.R., Smith, S.C., Sodt, A.J., Sunkin, S.M., Swanson, B.E., Vawter, M.P., Williams, D., Wohnoutka, P., Zielke, H.R., Geschwind, D.H., Hof, P.R., Smith, S.M., Koch, C., Grant, S.G.N., Jones, A.R., 2012. An anatomically comprehensive atlas of the adult human brain transcriptome. Nature 489, 391–399. https://doi.org/10.1038/nature11405.

Hawrylycz, M., Miller, J.A., Menon, V., Feng, D., Dolbeare, T., Guillozet-Bongaarts, A.L., Jegga, A.G., Aronow, B.J., Lee, C.-K., Bernard, A., Glasser, M.F., Dierker, D.L., Menche, J., Szafer, A., Collman, F., Grange, P., Berman, K.A., Mihalas, S., Yao, Z., Stewart, L., Barabási, A.-L., Schulkin, J., Phillips, J., Ng, L., Dang, C., Haynor, D.R., Jones, A., Van Essen, D.C., Koch, C., Lein, E., 2015. Canonical genetic signatures of the adult human brain. Nat. Neurosci. 18, 1832–1844. https://doi.org/10.1038/nn.4171.

Hodge, R.D., Bakken, T.E., Miller, J.A., Smith, K.A., Barkan, E.R., Graybuck, L.T., Close, J.L., Long, B., Johansen, N., Penn, O., Yao, Z., Eggermont, J., Höllt, T., Levi, B. P., Shehata, S.I., Aevermann, B., Beller, A., Bertagnolli, D., Brouner, K., Casper, T., Cobbs, C., Dalley, R., Dee, N., Ding, S.-L., Ellenbogen, R.G., Fong, O., Garren, E., Goldy, J., Gwinn, R.P., Hirschstein, D., Keene, C.D., Keshk, M., Ko, A.L., Lathia, K., Mahfouz, A., Maltzer, Z., McGraw, M., Nguyen, T.N., Nyhus, J., Ojemann, J.G., Oldre, A., Parry, S., Reynolds, S., Rimorin, C., Shapovalova, N. v, Somasundaram, S., Szafer, A., Thomsen, E.R., Tieu, M., Quon, G., Scheuermann, R.H., Yuste, R., Sunkin, S.M., Lelieveldt, B., Feng, D., Ng, L., Bernard, A., Hawrylycz, M., Phillips, J. W., Tasic, B., Zeng, H., Jones, A.R., Koch, C., Lein, E.S., 2019. Conserved cell types with divergent features in human versus mouse cortex. Nature 573, 61–68. https://doi.org/10.1038/s41586-019-1506-7.

Johnson, M.B., Kawasawa, Y.I., Mason, C.E., Krsnik, Z., Coppola, G., Bogdanović, D., Geschwind, D.H., Mane, S.M., State, M.W., Sestan, N., 2009. Functional and evolutionary insights into human brain development through global transcriptome analysis. Neuron 62, 494–509. https://doi.org/10.1016/j.neuron.2009.03.027.

Kalafatakis, K., Russell, G.M., Harmer, C.J., Munafo, M.R., Marchant, N., Wilson, A., Brooks, J.C.W., Thai, N.J., Ferguson, S.G., Stevenson, K., Durant, C., Schmidt, K., Lightman, S.L., 2016. Effects of the pattern of glucocorticoid replacement on neural processing, emotional reactivity and well-being in healthy male individuals: study protocol for a randomised controlled trial. Trials 17, 44. https://doi.org/10.1186/s13063-016-1159-x.

Kalafatakis, K., Russell, G.M., Harmer, C.J., Munafo, M.R., Marchant, N., Wilson, A., Brooks, J.C., Durant, C., Thakrar, J., Murphy, P., Thai, N.J., Lightman, S.L., 2018. Ultradian rhythmicity of plasma cortisol is necessary for normal emotional and cognitive responses in man. Proc. Natl. Acad. Sci. USA 115, E4091. https://doi.org/10.1073/pnas.1714239115. LP-E4100.

Kalafatakis, K., Russell, G.M., Lightman, S.L., 2019. Mechanisms in endocrinology: does circadian and ultradian glucocorticoid exposure affect the brain? Eur. J. Endocrinol. 180, R73. https://doi.org/10.1530/EJE-18-0853. –R89.

Kalafatakis, K., Russell, G.M., Ferguson, S.G., Grabski, M., Harmer, C.J., Munafò, M.R., Marchant, N., Wilson, A., Brooks, J.C., Thakrar, J., Murphy, P., Thai, N.J., Lightman, S.L., 2021. Glucocorticoid ultradian rhythmicity differentially regulates mood and resting state networks in the human brain: a randomised controlled clinical trial. Psychoneuroendocrinology 124, 105096. https://doi.org/10.1016/j.psyneuen.2020.105096.

Karst, H., Berger, S., Erdmann, G., Schütz, G., Joëls, M., 2010. Metaplasticity of amygdalar responses to the stress hormone corticosterone. Proc. Natl. Acad. Sci. USA 107, 14449. https://doi.org/10.1073/pnas.0914381107. LP – 14454.

Keller, J., Gomez, R., Williams, G., Lembke, A., Lazzeroni, L., Murphy Jr., G.M., Schatzberg, A.F., 2017. HPA axis in major depression: cortisol, clinical symptomatology and genetic variation predict cognition. Mol. Psychiatr. 22, 527–536. https://doi.org/10.1038/mp.2016.120.

Khan, S.M., Min, A., Gora, S., Houranieh, G.M., Campden, R., Robitaille, M., Trieu, P., Pétrin, D., Jacobi, A.M., Behlke, M.A., Angers, S., Hébert, T.E., 2015. Gβ4γ1 as a modulator of M3 muscarinic receptor signalling and novel roles of Gβ1 subunits in the modulation of cellular signalling. Cell. Signal. 27, 1597–1608. https://doi.org/10.1016/j.cellsig.2015.04.007.

Kuleshov, M.V., Jones, M.R., Rouillard, A.D., Fernandez, N.F., Duan, Q., Wang, Z., Koplev, S., Jenkins, S.L., Jagodnik, K.M., Lachmann, A., McDermott, M.G., Monteiro, C.D., Gundersen, G.W., Ma'ayan, A., 2016. Enrichr: a comprehensive gene set enrichment analysis web server 2016 update. Nucleic Acids Res. 44, W90–W97. https://doi.org/10.1093/nar/gkw377.

Levinson, A.J., Fitzgerald, P.B., Favalli, G., Blumberger, D.M., Daigle, M., Daskalakis, Z. J., 2010. Evidence of cortical inhibitory deficits in major depressive disorder. Biol. Psychiatr. 67, 458–464. https://doi.org/10.1016/j.biopsych.2009.09.025.

Li, J., Seidlitz, J., Suckling, J., Fan, F., Ji, G.-J., Meng, Y., Yang, S., Wang, K., Qiu, J., Chen, H., Liao, W., 2021. Cortical structural differences in major depressive disorder correlate with cell type-specific transcriptional signatures. Nat. Commun. 12, 1647. https://doi.org/10.1038/s41467-021-21943-5.

Lim, L.H.K., Pervaiz, S., 2007. Annexin 1: the new face of an old molecule. Faseb. J. 21, 968–975. https://doi.org/10.1096/fj.06-7464rev.

Luscher, B., Fuchs, T., Kilpatrick, C.L., 2011. GABAA receptor trafficking-mediated plasticity of inhibitory synapses. Neuron 70, 385–409. https://doi.org/10.1016/j.neuron.2011.03.024.

Lydersen, S., 2018. Balanced or imbalanced samples? Tidsskr. Nor. Laegeforen. 138 https://doi.org/10.4045/tidsskr.18.0539.

Neves, S.R., Ram, P.T., Iyengar, R., 2002. G protein pathways. Science 296, 1636–1639. https://doi.org/10.1126/science.1071550.

Mancarcı, B.O., n.d. Homologene.

Mancarci, B.O., Toker, L., Tripathy, S.J., Li, B., Rocco, B., Sibille, E., Pavlidis, P., 2017. Cross-laboratory analysis of brain cell type transcriptomes with applications to interpretation of bulk tissue data. eNeuro 4. https://doi.org/10.1523/ENEURO.0212-17.2017.

McArthur, S., Cristante, E., Paterno, M., Christian, H., Roncaroli, F., Gillies, G.E., Solito, E., 2010. Annexin A1: a central player in the anti-inflammatory and neuroprotective role of microglia. J. Immunol. 185, 6317–6328. https://doi.org/10.4049/jimmunol.1001095.

McReynolds, J.R., Doncheck, E.M., Li, Y., Vranjkovic, O., Graf, E.N., Ogasawara, D., Cravatt, B.F., Baker, D.A., Liu, Q.-S., Hillard, C.J., Mantsch, J.R., 2018. Stress promotes drug seeking through glucocorticoid-dependent endocannabinoid mobilization in the prelimbic cortex. Biol. Psychiatr. 84, 85–94. https://doi.org/10.1016/j.biopsych.2017.09.024.

Meijer, M., Keo, A., van Leeuwen, J.M.C., Dzyubachyk, O., Meijer, O.C., Vinkers, C.H., Mahfouz, A., 2021. Molecular characterization of the stress network in individuals at

risk for schizophrenia. Neurobiol Stress 14, 100307. https://doi.org/10.1016/j.ynstr.2021.100307.
Quintana, D.S., Rokicki, J., van der Meer, D., Alnæs, D., Kaufmann, T., Córdova-Palomera, A., Dieset, I., Andreassen, O.A., Westlye, L.T., 2019. Oxytocin pathway gene networks in the human brain. Nat. Commun. 10, 668. https://doi.org/10.1038/s41467-019-08503-8.
Réus, G.Z., Fries, G.R., Stertz, L., Badawy, M., Passos, I.C., Barichello, T., Kapczinski, F., Quevedo, J., 2015. The role of inflammation and microglial activation in the pathophysiology of psychiatric disorders. Neuroscience 300, 141–154. https://doi.org/10.1016/j.neuroscience.2015.05.018.
Rhen, T., Cidlowski, J.A., 2005. Antiinflammatory action of glucocorticoids — new mechanisms for old drugs. N. Engl. J. Med. 353, 1711–1723. https://doi.org/10.1056/NEJMra050541.
Ritchie, M.E., Phipson, B., Wu, D., Hu, Y., Law, C.W., Shi, W., Smyth, G.K., 2015. Limma powers differential expression analyses for RNA-sequencing and microarray studies. Nucleic Acids Res. 43 https://doi.org/10.1093/nar/gkv007 e47–e47.
Russell, G.M., Kalafatakis, K., Lightman, S.L., 2015. The importance of biological oscillators for hypothalamic-pituitary-adrenal activity and tissue glucocorticoid response: coordinating stress and neurobehavioural adaptation. J. Neuroendocrinol. 27, 378–388. https://doi.org/10.1111/jne.12247.
Sarabdjitsingh, R.A., Conway-Campbell, B.L., Leggett, J.D., Waite, E.J., Meijer, O.C., de Kloet, E.R., Lightman, S.L., 2010. Stress responsiveness varies over the ultradian glucocorticoid cycle in a brain-region-specific manner. Endocrinology 151, 5369–5379. https://doi.org/10.1210/en.2010-0832.
Shaw, G.T.W., Shih, E.S.C., Chen, C.-H., Hwang, M.-J., 2011. Preservation of ranking order in the expression of human housekeeping genes. PLoS One 6, e29314.
Smyth, G.K., 2004. Linear models and empirical bayes methods for assessing differential expression in microarray experiments. Stat. Appl. Genet. Mol. Biol. 3 https://doi.org/10.2202/1544-6115.1027. Article3.
Tasic, B., Yao, Z., Graybuck, L.T., Smith, K.A., Nguyen, T.N., Bertagnolli, D., Goldy, J., Garren, E., Economo, M.N., Viswanathan, S., Penn, O., Bakken, T., Menon, V., Miller, J., Fong, O., Hirokawa, K.E., Lathia, K., Rimorin, C., Tieu, M., Larsen, R., Casper, T., Barkan, E., Kroll, M., Parry, S., Shapovalova, N. v, Hirschstein, D., Pendergraft, J., Sullivan, H.A., Kim, T.K., Szafer, A., Dee, N., Groblewski, P., Wickersham, I., Cetin, A., Harris, J.A., Levi, B.P., Sunkin, S.M., Madisen, L., Daigle, T.L., Looger, L., Bernard, A., Phillips, J., Lein, E., Hawrylycz, M., Svoboda, K., Jones, A.R., Koch, C., Zeng, H., 2018. Shared and distinct transcriptomic cell types across neocortical areas. Nature 563, 72–78. https://doi.org/10.1038/s41586-018-0654-5.
Tasker, J.G., Herman, J.P., 2011. Mechanisms of rapid glucocorticoid feedback inhibition of the hypothalamic-pituitary-adrenal axis. Stress 14, 398–406. https://doi.org/10.3109/10253890.2011.586446.
Tierney, T., Christian, H.C., Morris, J.F., Solito, E., Buckingham, J.C., 2003. Evidence from studies on co-cultures of TtT/GF and AtT20 cells that Annexin 1 acts as a paracrine or juxtacrine mediator of the early inhibitory effects of glucocorticoids on ACTH release. J. Neuroendocrinol. 15, 1134–1143. https://doi.org/10.1111/j.1365-2826.2003.01111.x.
van Belle, G., 2008a. Statistical Rules of Thumb, second ed. Wiley, Hoboken, New Jersey.
van Belle, G., 2008b. Statistical Rules of Thumb, second ed. Wiley, Hoboken, New Jersey.
Technical White Paper, 2013. Microarray data normalization [WWW Document]. https://human.brain-map.org/static/download.
Wohleb, E.S., 2016. Neuron-microglia interactions in mental health disorders: “for better, and for worse. Front. Immunol. 7, 544. https://doi.org/10.3389/fimmu.2016.00544.
Xie, Z., Bailey, A., Kuleshov, M.V., Clarke, D.J.B., Evangelista, J.E., Jenkins, S.L., Lachmann, A., Wojciechowicz, M.L., Kropiwnicki, E., Jagodnik, K.M., Jeon, M., Ma'ayan, A., 2021. Gene set knowledge discovery with Enrichr. Curr Protoc 1, e90. https://doi.org/10.1002/cpz1.90.
Zhou, Y., Zhou, B., Pache, L., Chang, M., Khodabakhshi, A.H., Tanaseichuk, O., Benner, C., Chanda, S.K., 2019. Metascape provides a biologist-oriented resource for the analysis of systems-level datasets. Nat. Commun. 10, 1523. https://doi.org/10.1038/s41467-019-09234-6.